



1 **Delineating small karst watersheds based**  
2 **on digital elevation model and**  
3 **eco-hydrogeological principles**  
4

5 G.J. Luo <sup>a,b,c</sup>, S.J. Wang <sup>a,\*</sup>, X.Y. Bai <sup>a</sup>, X.M. Liu <sup>a</sup>, A.Y. Cheng <sup>d</sup>

6 <sup>a</sup> State Key Laboratory of Environmental Geochemistry, Institute of Geochemistry, Chinese  
7 Academy of Sciences, Guiyang 550081, China

8 <sup>b</sup> University of Chinese Academy of Sciences, Beijing 100049, China

9 <sup>c</sup> Institute of agricultural ecology and rural development, Guizhou Normal College, Guiyang  
10 550018, China

11 <sup>d</sup> Puding Karst Ecosystem Observation and Research Station, Chinese Academy of Sciences,  
12 Anshun 561000, China

13 \* Corresponding Author: Shijie Wang, Email: wangshijie@vip.gyig.ac.cn  
14  
15

16 **Summary:** Dominated by specific eco-hydrogeological backgrounds, a small watershed  
17 delineated by using the traditional method is always inauthentic in karst regions because it cannot  
18 accurately reflect the eco-hydrological process of the dual structure of the surface and subsurface.  
19 This study proposes a new method for the delineation of small watersheds based on digital  
20 elevation model (DEM) and eco-hydrogeological principles in karst regions. This method is  
21 applied to one section of the tributary area (Sancha River) of the Yangtze River in China. By  
22 comparing the quantity, shape, superimposition, and characteristics of the internal hydrological  
23 process of a small watershed extracted by using the digital elevation model with that extracted by  
24 using the proposed method of this study, we conclude that the small karst watersheds extracted by  
25 the new method accurately reflect the hydrological process of the river basin. Furthermore, we  
26 propose that the minimum unit of the river basin in karst regions should be the watershed whose  
27 exit is the corrosion-erosion datum and a further division of watershed may cause a significant  
28 inconsistency with the true eco-hydrological process.  
29



30 **Key words:** delineation of karst watershed; corrosion–erosion datum; DEM; eco-hydrogeology;

31 Sancha River

32

### 33 **1. Introduction**

34

35 Karst is the term used to describe a special type of landscape containing caves and extensive  
36 underground water systems that is developed particularly on soluble rocks, such as limestone,  
37 marble, and gypsum (Ford and Williams, 2007). By the action of lithology and tectonics, soluble  
38 carbonate rocks form a double-deck structure by corrosion and erosion in the surface and  
39 subsurface. Rain falls into shafts and sinks, thus causing the subsurface to crack rapidly,  
40 particularly in several karst mountain areas. The water infiltration coefficient is up to 0.8 (Liu and  
41 Li, 2007; Meng and Wang, 2010). Thus, karst eco-hydrological processes are characterized as the  
42 dual structure of the surface and subsurface (Yang, 1982). The amounts of surface runoff and soil  
43 loss on karst hill slopes are small compared with non-karst areas because of the dual hydrological  
44 structure of karst regions, including ground and underground drainage systems. Most rainfall  
45 water is transported underground through limestone fissures and fractures, whereas only a small  
46 proportion of rainfall water is transported in the form of surface runoff (Peng and Wang, 2012).  
47 Moreover, karst also provides diverse subterranean habitats, including epikarst, cave streams, drip  
48 pools, springs, and interstices (Bonacci et al., 2009). In karst regions a large number of studies  
49 have focused on hydrology, soil erosion, water resources, and ecosystems basing on the watershed  
50 unit (Rimmer and Salingar, 2006; Navas et al., 2013; McCormack et al., 2014). However, many  
51 studies don't assess accuracy of the scope of the watershed, or several only assess the catchment  
52 scope for a single spring in the watershed (key papers are summarized in Table 1 in relation). In  
53 summary, a small watershed is the basic unit between ecosystem management and basic science  
54 research in karst areas (Xiong et al., 2014; Doglioni et al, 2012) and not papers illustrated  
55 delineating karst watersheds in geographical area scale considering the karst double-deck structure  
56 in the surface and subsurface.

57

58

59



60

Table 1

Summary of relevant field studies basing on watershed scale in karst areas. Not all papers illustrated data and method to map the scope of the studied watershed and these are denoted with a N/A representing 'not applicable' in the relevant part of the 'Data / Method to map the scope of the watershed' column. In the 'Key results' column assess accuracy of the scope of the watershed is identified. Many studies do not assess and N/A directly follows the code in such cases.

Study	Field	Location / watershed / study size	Data / Method to map the scope of the watershed	Key results
1 - Majone et al. (2004)	Karst runoff	Northeastern Italy / Centonia and Prese Val / 20.6 km <sup>2</sup> and 1.96 km <sup>2</sup>	N/A / N/A	N/A
2 - Rimmer and Salinger (2006)	Precipitation-streamflow model	Hermon mountain, Jordan River / Dan, Snir and Hermon / 252 km <sup>2</sup> , 118 km <sup>2</sup> , 106 km <sup>2</sup>	DTM / N/A	N/A
3 - Bailly-Comte et al. (2009)	Hydrodynamics	Near Montpellier, Southern France / Coulazou River / 61 km <sup>2</sup>	N/A / N/A	N/A
4 - Mayaud et al. (2014)	Groundwater hydraulics	Styria, Austria / Lurbach / 23 km <sup>2</sup>	Geological map / Investigation	Surface Lurbach stream: 15 km <sup>2</sup> , subsurface karstified unit: 8 km <sup>2</sup>
5 - Malard et al. (2015)	Groundwater hydraulics	Northeastern Switzerland / Beuchire-Creugenat (BC) and Bonnefontaine-Voyeboeuf (BV) / 58 km <sup>2</sup> and 19 km <sup>2</sup>	Geological map / Investigation	BC: Autogenic parts 50.5 km <sup>2</sup> and Allogenic parts 6.5 km <sup>2</sup> , respectively BV: 16.5 km <sup>2</sup> and 2.5 km <sup>2</sup>



6 - Yue et al. (2015)	Nitrate sources and transformation processes	Southwestern China / Houzhai / 81 km <sup>2</sup>	N/A / N/A	N/A
7 - Wicks (1997)	Groundwater hydraulics	Central Missouri, USA / Bonne Femme / 31.6 km <sup>2</sup>	N/A / Surface-water drainage patterns, topography, and dye tacing	Surface stream: 21.3 km <sup>2</sup> , subsurface stream: 10.3 km <sup>2</sup>
8 - Ravbar and Goldscheider (2009)	Groundwater vulnerability mapping	Southwestern Slovenia / Podstenjšek / 9.1 km <sup>2</sup>	N/A / N/A	N/A
9 - Navas et al. (2013)	soil redistribution	Spanish Pyrenees / Estanque de Arriba Lake / 0.8 km <sup>2</sup>	DEM / N/A	N/A
10 - McCormack et al. (2014)	groundwater discharge and nutrient	Western Ireland / Gort Lowlands / 483 km <sup>2</sup>	N/A / N/A	N/A



62 Watersheds, which have boundaries shaped by geomorphic and physical processes rather than  
63 political borders (Hollenhorst et al, 2007), have become more accepted as the basic unit of water  
64 resource management and ecological protection (NRC, 1999). The digital elevation model (DEM)  
65 provides a solid technical foundation for the development of a digital hydrological model that can  
66 be used for watershed extraction and topographic analysis (Mantelli et al, 2011; Li and Hao, 2003).  
67 Basin delineation is generally based on digital morphology and consists of two major steps:  
68 removal of all pits within the model by using an original morphological mapping, delineation of  
69 the topographic basins by using morphological thinning with specific structuring elements (Soille  
70 and Ansoult, 1990). The DEM is one of the many products available for public use that provide  
71 information regarding new datasets for drainage extraction and watershed delineation (Hancock et  
72 al., 2006). Therefore, extracting the topographic information of watersheds, such as ridge lines,  
73 stream networks, and watershed area, from DEMs has been investigated since the early 1970s  
74 (Peucker and Douglas, 1975; Gallant and Hutchinson, 2009). In previous studies, the flow  
75 accumulation value (the number of grid cells that drain into a particular cell) was calculated to  
76 establish drainage networks (Marks et al., 1984; O'Callaghan and Mark, 1984). The procedure of  
77 partitioning watersheds within the DEM consists of three phases, namely, delineation of a channel  
78 network, delineation of a drainage divide network, and labeling of the basins by assigning each  
79 pour point a unique positive integer and drainage direction (Band, 1986). Thereafter, the interior of  
80 each basin is labeled according to its pour point identifier (Benosky and Merry, 1995). In recent  
81 years, automated watershed extraction based on DEM has been extensively used, particularly the  
82 combination of DEM with advances in geographic information system (GIS) techniques, as a tool  
83 for watershed extraction (García and Camarasa, 1999; Ahamed et al., 2002; Vogt et al., 2003;  
84 Hollenhorst et al., 2012; Qiu and Zheng, 2012).

85 China has approximately  $3.44 \times 10^6$  km of karst areas, which is approximately 36% of its total  
86 land area and 15.6% of all  $22 \times 10^6$  km karst areas in the world (Jiang et al., 2014). The  
87 continuously distributed karst region, which is mostly located in eight provinces of southwest  
88 China (Guizhou, Yunnan, Guangxi, Chongqing, Sichuan, Hunan, Hubei, and Guangdong), is one  
89 of the most extensive and well-developed karst landscapes of the world (Wang et al., 2004).  
90 Rocky desertification, which is used to characterize the processes that transform a karst area  
91 covered by vegetation and soil into a rocky landscape almost devoid of soil and vegetation (Yan,



92 1997), is the most serious ecological problem in southwest China. Therefore, a comprehensive  
93 harness outline for rocky desertification in karst regions (2006–2015) in southwest China projects  
94 approved by the State Council of the People’s Republic of China and funded by the Chinese  
95 government at different levels has resulted in significant progress in ecological restoration in  
96 recent decades (Xiao et al., 2014). Small watershed is a basic unit to implement these projects. We  
97 cannot always rely directly on automatically extracted watersheds, particularly in regions with  
98 internal drainage (e.g. karst regions) or in plateau areas, where filling depressions can produce  
99 large uncertainties in the extracted networks and watershed boundaries (Khan et al., 2014).  
100 Automated watershed extraction based on the DEM of the surface morphological characteristic of  
101 the earth seems necessary to improve the methods used. Automatically delineated surface small  
102 watersheds do not always show close agreement with subsurface small watersheds because the  
103 subsurface hydrological process is not considered, thus leading to the distortion in the basin  
104 boundary and hydrological and ecological processes. This phenomenon further restricts scientific  
105 water resource management and ecological restoration projects. Thus, the accurate extraction of  
106 karst watersheds (KW) is important.

107 This study aims to characterize and compare the proposed extraction method of small  
108 watersheds in karst areas with the traditional watershed extraction method that topographic small  
109 watersheds are delineated automatically (ATW). We select a typical karst area to extract the KW.  
110 The study site is a section of Sancha River upstream of Wujiang River, a branch of the Yangtze  
111 River in China.

112

## 113 2. Study site and materials

114

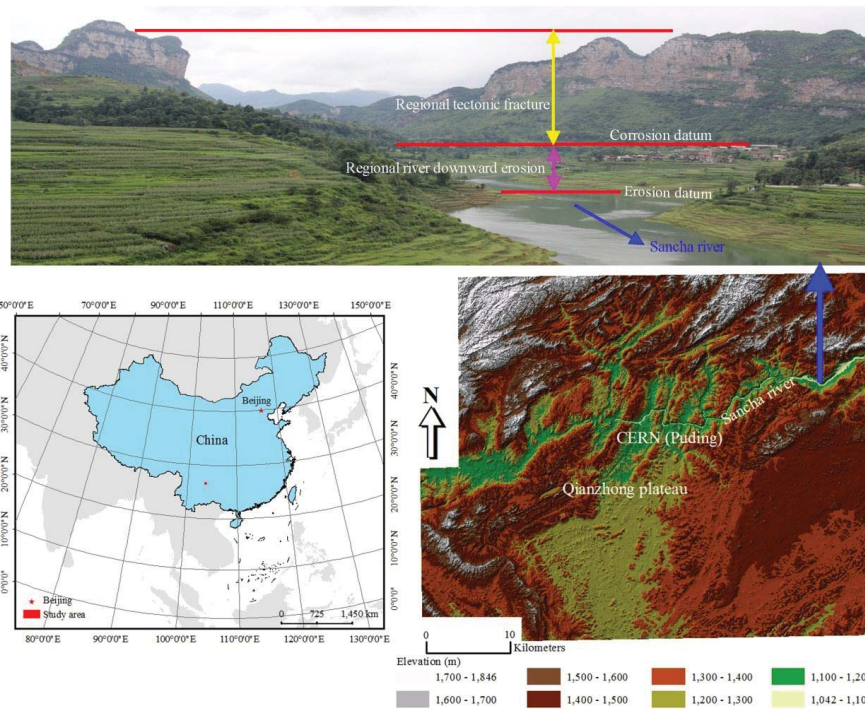
### 115 2.1. Study site

116

117 Our study area on the Qianzhong Plateau ( $A = 2,193.14 \text{ km}^2$ ) is the part of the Sancha River  
118 upstream of the Wujiang River, a branch of the Yangtze River in China (Fig. 1). The elevations of  
119 the study area vary between 1,042 and 1,846 m asl. The climate type is north subtropical monsoon,  
120 with a high mountain influence. In recent decades, the mean annual rainfall amount is 1,400 mm/a  
121 and peaks in the summer season during storm events and the annual average temperature is 15.6



122 deg. C from 1961 to 2006. Strata from the Cambrian of the Lower Paleozoic Erathem to the  
 123 Quaternary of the Cenozoic Erathem, except Silurian, Jurassic, and Cretaceous, all exhibit  
 124 exposures. Among these exposures, the carbonate rocks of Permian and Triassic are most widely  
 125 distributed, accounting for greater than 90% of the study area (Table 2). Karst develops intensively.  
 126 Thus, karst landforms, such as dolines, karren zones, and dry valley, are visible on the plateau,  
 127 thus indicating that karstification is relatively high in the study zone with 23 underground rivers.  
 128 The Yelanghu Reservoir, constructed in the study area in 1994, has become one of the main  
 129 freshwater sources in Anshun, which supply drinking water to the city (Zhang et al, 2011). The  
 130 Sancha River is the largest river in the study area and is considered the erosion datum of the study  
 131 area.



132  
 133

Fig. 1. Location and topography of the study area.

Table 2. Quantity of all types of strata outcropped in the study area

Geological time	Percentage of strata outcropped (%)



---

Cenozoic	Quaternary	3.4
	Paleogene	1.06
Mesozoic	Triassic	64.04
	Dyas	26.92
Upper Paleozoic	Carboniferous	5.91
	Devonian	0.5
Lower Paleozoic	Ordovician	0.03
	Cambrian	2.14

---

134

## 135 2.2. Materials

136

137 The data employed in this study include 1:50,000 digital line graphic (DLG) data provided by  
138 the State Key Laboratory of Environmental Geochemistry (transformed into DEM, with a  
139 resolution of 30 m, by using ArcGIS), geological data, hydrogeological data obtained through  
140 hydrogeological mapping, hydrogeological drilling, water quality tracing experiment based on  
141 geophysical prospecting, and high-resolution remote sensing image data (resolution of <2 m). In  
142 2012, precipitation in the study area is the data provided by the online observation of ecosystems  
143 and by research stations in China (Chinese Ecosystem Research Network (CERN), Puding). The  
144 aforementioned data sources are used in ArcGIS to establish a coordinate system that can be used  
145 to conduct spatial analysis. After the indoor extraction of KW based on the method previously  
146 presented, we conducted considerable field work to verify the boundary of small watershed on  
147 site.

148

## 149 3. Method

150

151 In this study, the delineation of KW is completed by the following five steps:

152 (i) ATW is delineated by using the hydrological tools in ArcGIS 10 (ESRI 2010).

153 (ii) Regional corrosion–erosion datum and exit of watershed are determined.

154 (iii) The trunk stream of the dual structure of the surface and underground is determined.

155 (iv) The flow direction in the permeable stratum of karst carbonate in the region is determined.



156 (v) The divide of watershed is corrected and KW extraction is completed.

157

### 158 3.1. Extraction of ATW

159

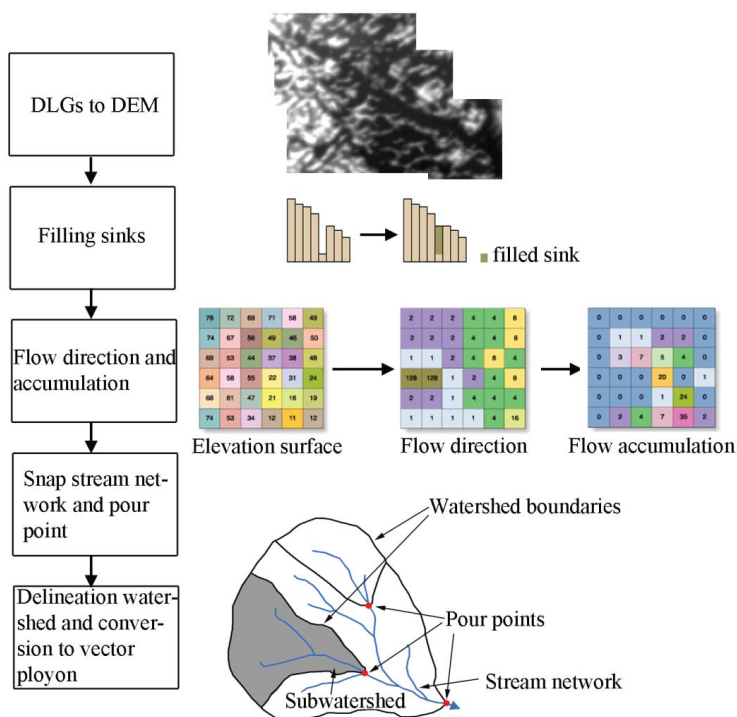
160 By adopting the traditional method of automatic extraction, this step is completed by using the  
161 hydrological tools available in ArcGIS (Martz and Garbrecht, 1999). The basic process is as  
162 follows (shown in Fig. 2):

163 In ArcGIS, TIN is established by using the digital line graphic (DLG) data and is converted to  
164 DEM data, but DEM data can also be obtained from existing data (such as ASTER DEM and  
165 SRTM DEM). Thereafter, flow distribution is conducted by using the commonly adopted D8  
166 algorithm (Mark, 1984; O’Callaghan and Mark, 1984). However, in actual DEM products, grids  
167 around the karst regions are higher than the depressions because of false data or the existence of  
168 “pits” or “sinks” in actual terrain. This phenomenon results in the retention of runoffs in  
169 depressions. Consequently, the extracted river network is discontinued and deviation errors occur  
170 in the flow direction and river network (Nikolakopoulos et al., 2006; Jiang et al., 2014; Tarboton et  
171 al., 1991). Therefore, the pretreatment of DEM data is necessary to fill the depressions in the data.  
172 The filling of sinks is also shown in Fig. 2. After this process, the elevation value of the grid of the  
173 depression is equal to the elevation value of the surrounding lowest point. By modifying the  
174 elevation value specified previously, the elevation values of all grids in the DEM are larger than or  
175 equal to that of the lowest outlet. In this manner, a DEM “with hydrological meaning” is generated  
176 and the continuity of the natural water system of the watershed extracted from DEM data can be  
177 ensured (Li et al., 2003).

178 After filling the depressions, the elevation of each DEM grid can be compared with its adjacent  
179 grids in 8 directions. The direction with the steepest slope is the direction of the runoff in this grid  
180 (Kiss, 2004; Jenson and Domingue, 1988). In ArcGIS, grids obtained after the calculation of the  
181 flow direction are marked as 1, 2, 4, 8, 16, 32, 64, and 128 to record the different flow directions  
182 of grids (the flow direction is also shown in Fig. 2). On the basis of the determined flow directions  
183 of grids, the area of the upstream catchment of this grid is determined by calculating the number  
184 of grids whose upstream catchment flows directly or indirectly to the designated grid (the flow  
185 accumulation is also shown in Fig. 2) (Jensen, 1991). After generating an output raster of flow



186 accumulation, the threshold of the grid where flows accumulated is selected as the area threshold  
187 of the upstream feeding area on the basis of the characteristics of climate in a certain region. The  
188 grid whose threshold is equal to the area threshold is adopted as the initial point of the watercourse.  
189 Grids with thresholds greater than the area threshold constitute the watercourse (Qiu et al, 2012).  
190 Furthermore, watershed and subwatershed pour points can be defined by using the accumulated  
191 area raster (the snap stream network and pour point are shown in Fig. 2). Thereafter, the watershed  
192 can be delineated and the watershed boundary can be converted to a vector polygon by using GIS  
193 tools (Khan et al., 2014).



194

195 Fig. 2. ATW delineation process by using the hydrological tools available in ArcGIS (from ArcGIS

196

help).

197

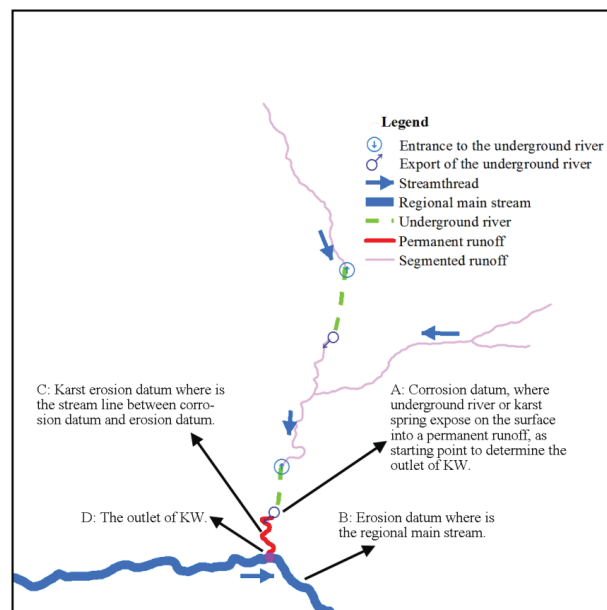


198 **3.2. Determination of the regional corrosion–erosion datum and exit of watershed**

199

200 Influenced by regional tectonic activities, the datum plane significantly affects the hydrological  
201 and geomorphic processes within a certain region (Fitzpatrick, 1998). The erosion datum is  
202 usually at the level of the adjacent large river instead of the sea level in most parts of a karst region.  
203 As such, the erosion datum is associated with the sea level through the trunk stream (Li and Cui,  
204 2004). The regional tectonic uplift and strong downcutting of the river cause the formation of  
205 relatively independent water-bearing blocks locally. In most cases, independent recharge, runoff,  
206 and discharge areas exist in each block, which leads to the exposure of subterranean rivers or karst  
207 springs around the discharge datum plane in karst regions (Yang, 1982). As a result, the place  
208 where subterranean rivers or karst springs is exposed can be turned into a perpetual open channel  
209 because the corrosion datum of this area in karst regions can be used to determine the exit of  
210 watersheds (shown in Fig. 3A). The main watercourse of a large river in the region is considered  
211 the regional erosion datum line (shown in Fig. 3B). In this manner, the line linking corrosion  
212 datum and erosion datum is the regional corrosion–erosion datum line (shown in Fig. 3C). In  
213 watershed management, the intersection of the corrosion–erosion datum line and the main  
214 watercourse of the large river is considered the exit of the KW (shown in Fig. 3D).

215





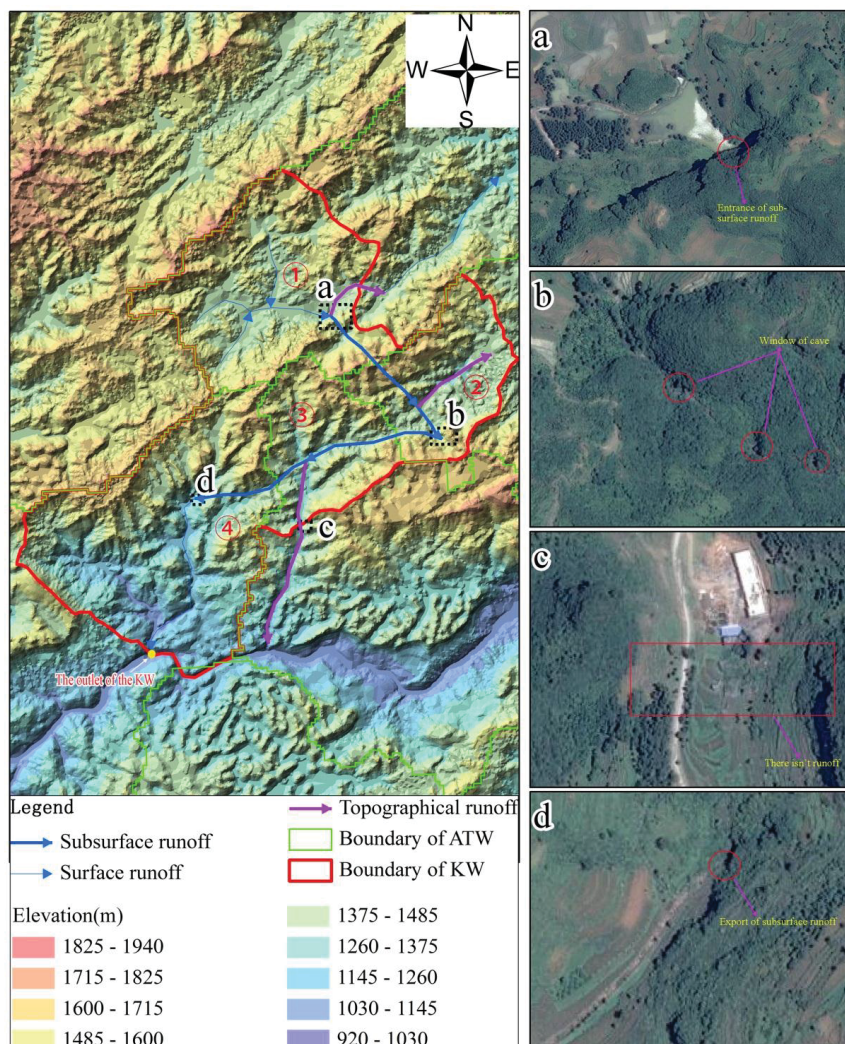
216 Fig. 3. Schematic used to determine the outlet of KW.

217

218 **3.3. Determination of the trunk stream of the dual structure of the surface and underground**  
219 **in KW**

220

221 As stated in Section 3.2, the watercourse of the large river, which can be extracted automatically  
222 based on the DEM, is the trunk stream of the watershed in the downstream area of the regional  
223 corrosion–erosion datum in karst regions. By contrast, the main watercourse is often characterized  
224 by the alteration of open channels and subterranean streams in the upstream area of the  
225 corrosion–erosion datum because of the effects of the lithologic characteristics and structure of  
226 stratum, fault, and folding. In the area of subterranean streams, the error rate of the automatic  
227 extraction of trunk stream based on the DEM is high. Thus, the manual correction of the trunk  
228 stream of ATW can be conducted from the upstream watercourse to the exit of KW by using  
229 terrain data, high-resolution images, and hydrogeological data. The correction process is shown on  
230 the left of Fig. 4. In the upstream area of ①<sup>#</sup> ATW featuring clastic rocks, the trunk stream is the  
231 surface runoff that enters the carbonatite area at a. The trunk stream turns into a subterranean river  
232 and flows to the ②<sup>#</sup> ATW area. At b, the subterranean river encounters the water-resisting layer of  
233 clastic rocks and flows to ③<sup>#</sup> ATW area through sunken pipes. Finally, the subterranean river  
234 flows out of the surface at b in the ④<sup>#</sup> ATW area. The trunk stream reaches the exit of the KW  
235 and enters the watercourse of the regional large river (erosion datum). According to the  
236 high-resolution images, no overland runoffs exist in the automatically extracted areas where the  
237 trunk stream flows through in the eastward direction of a in the ①<sup>#</sup> ATW, the eastward direction  
238 of b in the ②<sup>#</sup> ATW, and the southward direction of c in the ③<sup>#</sup> ATW. The hydrological  
239 processes of these areas are dominantly underground processes. Thus, manual correction is  
240 necessary on the topographic trunk stream extracted automatically in these areas to obtain the  
241 trunk stream on the basis of the dual structure of the surface and underground in the KW.



242

243 Fig. 4. Process used to determine the trunk stream of the dual structure of the surface and

244 underground in KW.

245

246 **3.4. Determination of the flow direction in the permeable strata of karst carbonatite in the**  
 247 **regions where trunk stream flows through**

248

249 After the determination of the trunk stream of the surface and underground in KW, determining  
 250 the flow direction of each hydrogeological unit in the area it flows through becomes an important



251 step for the extraction of KW. In non-karstic terrains, groundwater divides are assumed to directly  
252 underlie the surface topographic divides as determined from contour maps and aerial photographs  
253 (Ford and Williams, 2007). However, in karst areas, groundwater flow is significantly independent  
254 of topography but is often guided by geological formations and structures (Nico and David, 2007).  
255 Therefore, in areas without carbonatite, the flow direction is determined on the basis of the surface  
256 terrain. By contrast, in carbonatite areas, the flow direction is determined by considering the  
257 lithologic characteristics and the combination of strata, fault, and structure and by conducting  
258 geophysical survey, tracing experiment, and model simulation. On this basis, the distribution of  
259 watershed in the area with permeable strata in karst carbonatite is determined.

260

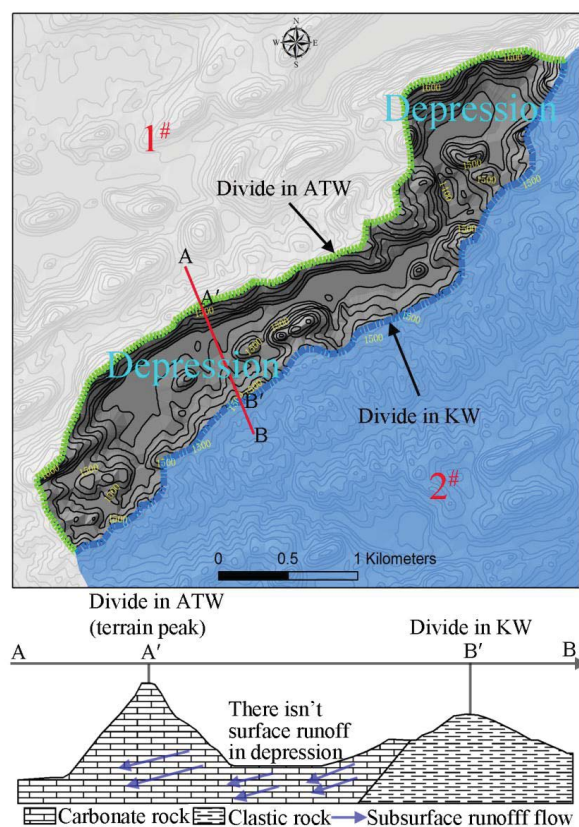
### 261 3.5. Correction of the divide of ATW

262

263 After completing the steps presented in Section 3.4, the watershed distribution of all karst  
264 hydrogeological units is almost completely determined. Corrections on several divides extracted  
265 automatically are imperative to enable the boundary of the dividing area to reflect the karst  
266 hydrological process more accurately. Two conditions must be considered in the process of  
267 correction. (1) The divide runs through areas featuring clastic rocks (not carbonatite) with  
268 water-resisting layers or slopes where the terrain changes significantly. Considering the fact that  
269 the hydrological process of these areas is mainly characterized by surface runoffs, the watershed  
270 boundary of KW is considered the watershed boundary of ATW, i.e., correction on the  
271 automatically extracted divide is not needed. (2) In carbonatite areas characterized by underground  
272 corrosion where vertical permeation and subsurface runoff are the dominant hydrological  
273 processes (negative relief develops well in these areas and peak cluster depression is the main  
274 topographic feature), correction of ATW boundary and watershed distribution is completed by  
275 using hydrogeological data and high-resolution images and by using the flow direction determined  
276 in Section 3.4. In this regard, an example is shown in Fig. 5. A depression with no surface runoff is  
277 observed in the dividing area between KW 1<sup>#</sup> and KW 2<sup>#</sup>, and the hydrological process is  
278 absolutely different from that of surface terrain. Underground runoffs in the depression flows  
279 through A' (terrain peak) and sunken pipes in karst carbonatite areas and accumulates in KW 1<sup>#</sup>.  
280 However, the true divide goes through the water-resisting layer of clastic rocks where B' is located.



281 Accordingly, we conduct manual correction on the watershed divide on the basis of the features of  
282 the underground hydrological process.



283

284 Fig. 5. Correction divide based on the ATW boundary in the depression area.

285

## 286 4. Results

287

### 288 4.1 Comparison of the topographic characteristics of ATW and KW

289

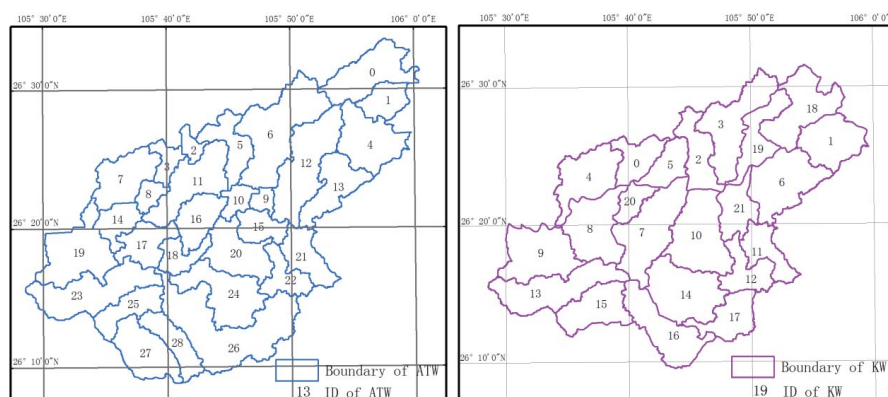
290 From the perspective of quantity, 22 small KWs are extracted in the study area. Compared with those  
291 based on DEM, the number of watersheds was reduced by seven (Fig. 6), a decrease of 24%. For the  
292 watershed boundary, the total length of the boundaries of small watersheds on the surface obtained  
293 based on the DEM in the study area is 1,381.47 km. The total length of the boundaries of KWs is



294 1,004.18 km. The length of the boundaries shared by these two types is 394.36 km, accounting for 28.5%  
 295 of surface watershed boundaries and 39.27% of KW boundaries.

296 In terms of the superimposition of watersheds, the number of watersheds that reached the level  
 297 of coupling is nine in ATW and KW. The number of watersheds without any coupling is also nine,  
 298 and the number of approximate coupling is four (shown in Table 3). Furthermore, except for  
 299 watershed 3#, at least two pairs of superimposition of surface watersheds are observed in all the  
 300 other small KWs.

301 In conclusion, significant differences in the number of watersheds, boundary, and  
 302 superimposition exist between ATW and KW because of the influence of specific  
 303 eco-hydrogeological background in karst regions.



304  
 305 Fig. 6. A quantitative contrast between KW and ATW.

306 Table 3. Evaluation of the spatio-superimposed relationship between KW and ATW

ID of KW	Area	ID of ATW (Fig. 6)	Maximum of ATW	Percentage	Type
0	29.91	2, 3, 11, 8	15.31	51.19	No coupling
1	48.35	1, 4	47.03	97.28	Coupling
2	37.14	5, 6, 10, 11, 9	27.93	75.20	Segmental coupling
3	65.46	6	65.46	100.00	Coupling
4	52.80	7, 8, 14	45.92	86.95	Segmental coupling
5	26.86	11	26.86	100.00	Coupling
6	65.57	4, 12, 13	42.99	65.56	No coupling



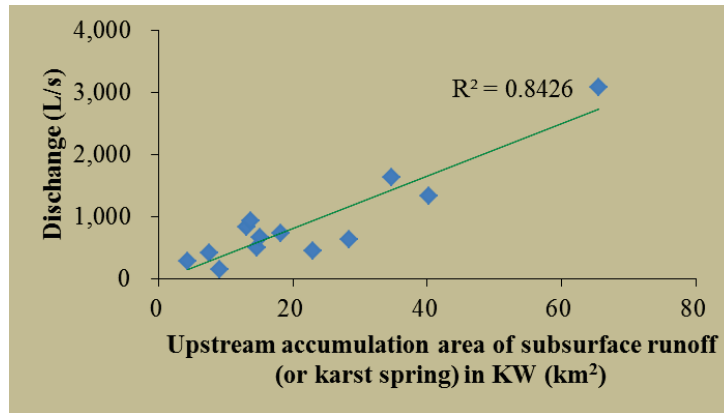
7	72.98	5, 10, 16, 17, 18, 24, 26, 11	33.41	45.78	No coupling
8	59.29	7, 8, 14, 17, 19, 23, 11	25.11	42.35	No coupling
9	62.32	19, 23	56.83	91.20	Coupling
10	71.73	9, 10, 16, 20, 24, 15	46.97	65.48	No coupling
11	30.35	21, 22	30.28	99.76	Coupling
12	31.45	15, 20, 22, 26, 21	26.22	83.40	Segmental coupling
13	66.39	23, 26	65.51	98.67	Coupling
14	67.80	20, 24, 26	55.12	81.31	Segmental coupling
15	44.71	23, 25, 28, 27	31.09	69.53	No coupling
16	57.16	25, 26, 28	55.86	97.71	Coupling
17	34.92	22, 24, 26	33.96	97.24	Coupling
18	59.23	0, 1, 12, 13, 4	23.75	40.10	No coupling
19	37.96	6, 9, 12	21.70	57.17	No coupling
20	17.07	3, 8, 11	16.60	97.27	Coupling
21	32.28	9, 12, 20, 15	14.45	44.77	No coupling

Notes: no coupling–percentage <70; segmental coupling  $70 \leq$  percentage < 90; coupling  $90 \leq$  percentage  
 307

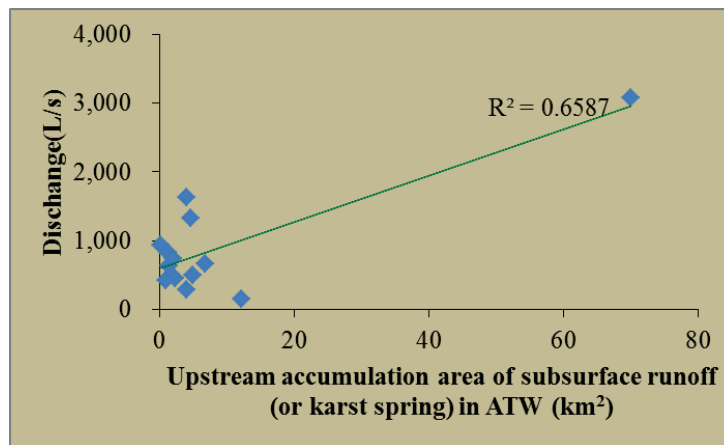
#### 308 4.2. Comparison of the features of the hydrological process between ATW and KW

309

310 The linear correlation between the water flow of subsurface runoff (or karst spring) in normal  
 311 seasons (from May to October), which is one of the 13 rivers with water flow obtained previously,  
 312 and the area of the upstream catchment is examined. In KW, the linear correlation coefficient ( $R^2$ )  
 313 between the water flow in normal seasons and the area of the upstream catchment is 0.84, which is  
 314 evidently higher than 0.66, the coefficient of ATW (Fig. 7). In addition, Table 4 shows the  
 315 proportions of atmospheric precipitation in the upstream catchment area of 13 subterraneous rivers  
 316 (or karst springs) that are converted into subsurface runoffs. The values of 2#, 3#, 4#, 5#, 6#, 7#,  
 317 8#, 9#, 10#, 11#, and total  $R_{ATW}$  are all greater than 100, thus indicating that the upstream  
 318 catchment areas extracted automatically are small. Accordingly, the  $R_{KW}$  values of 13 subsurface  
 319 runoffs (or karst springs) are all less than 100, thus indicating that the small KW that we extracted  
 320 is reasonable.



321



322

323 Fig. 7. Correlation between the discharge of subsurface runoffs (or karst springs) and the upstream  
 324 watershed area in KW and ATW.

325

326 Table 4. Infiltration efficiency from the atmospheric precipitation in the upstream catchment area  
 327 of subsurface runoffs (or karst springs) ( $R_{ATW}$  in ATW and  $R_{KW}$  in KW, %). Notes:  $R_{KM} =$   
 328  $\frac{D}{A_{KM}} \times T \times r$  and  $R_{ATM} = \frac{D}{A_{ATM}} \times T \times r$ , where  $T$  is the total number of seconds from May  
 329 to October;  $r$  is the factor for unit conversion in  $D$ ,  $A$ ,  $T$ , and  $P$ ;  $p$  is 1,197.2 mm, which is the  
 330 hourly rainfall amount recorded by the automatic weather station in CERN (Puding) from May to  
 331 October in the study area.

No.	$D$	$A_{KW}$	$A_{ATW}$	$R_{ATW}$	$R_{KW}$
-----	-----	----------	-----------	-----------	----------



	Discharge (L/s)	Upstream accumulation area of subsurface runoff (or karst spring) in KW (km <sup>2</sup> )	Upstream accumulation area of subsurface runoff (or karst spring) in ATW (km <sup>2</sup> )	The percentage of precipitation into subsurface runoff in ATW	The percentage of precipitation into subsurface runoff in KW
1 <sup>#</sup>	3,076.00	65.57	69.92	58.42	62.29
2 <sup>#</sup>	1,634.20	34.69	4.01	540.96	62.56
3 <sup>#</sup>	1,331.10	40.31	4.61	383.29	43.85
4 <sup>#</sup>	940.20	13.72	0.07	16,970.80	90.97
5 <sup>#</sup>	832.51	13.05	1.16	956.17	84.72
6 <sup>#</sup>	740.00	18.22	1.93	508.47	53.94
7 <sup>#</sup>	660.60	15.14	6.76	129.73	57.92
8 <sup>#</sup>	632.49	28.30	1.27	663.94	29.68
9 <sup>#</sup>	496.40	14.57	4.95	133.25	45.24
10 <sup>#</sup>	450.00	22.94	2.31	258.45	26.05
11 <sup>#</sup>	424.00	7.48	0.89	634.45	75.30
12 <sup>#</sup>	279.80	4.21	3.93	94.51	88.18
13 <sup>#</sup>	157.50	9.01	12.19	17.16	23.22
Sum	11,654.80	287.22	113.99	135.77	53.88

332

333 **5. Discussion**

334

335 **5.1. The novel approach of delineation KW**

336

337 The automatic delineation of watersheds is extensively accepted and applied by hydrologists,  
 338 geologists, and ecologists internationally because of the convenience in the acquisition of data



339 source and automation in the extraction process (Verdin and Verdin, 1999). However, in karst  
340 areas, wherein the eco-hydrogeological background is complex and significant differences exist in  
341 the dual structure of the surface and underground (Yang, 1982). This study has presented a novel  
342 approach to overcome faults of the traditional method of delineation watersheds in karst areas, by  
343 combining hydrogeological background and DEMs. The method proposed in this study not only  
344 had similar advantages of accurate expression of terrain and quick automation as the traditional  
345 automatic extraction method but also considered the specific eco-hydrogeological background in  
346 karst areas.

347 The multiple methods from the geography, topography, hydrology and hydrogeology were used  
348 conformably in the five steps of delineation KW. The work extends previous studies on watershed  
349 delineation using 3S (GIS, RS and GPS) and digital terrain data (Hollenhorst et al., 2007; Seyler et  
350 al., 2009). In these studies watershed delineation has the following advantages: (i) the DEMs data  
351 (e.g. the Shuttle Radar Topography Mission DEM and the Advanced Spaceborne Thermal  
352 Emission and Reflection Radiometer – Global Digital Elevation Model) is easy available (Jarihani  
353 et al., 2015); and (ii) Surface morphology analysis based on DEMs is accurate in the digital  
354 mapping to ditch, slope, mountain divide and drainage network, with the advantages of high  
355 automation and wide spatial scale from the global to the nano - or microscales (Wilson and Gallant,  
356 2000).

357 On the other hand, in the research fields of karst hydrology and karst hydrogeology, the study of  
358 watershed delineation most concentrated on delineation the catchment area of a single spring  
359 (Table 1) (e.g. Fontaine de Vaucluse Spring in the southeastern karst region of France; St. Ivan  
360 karst spring in the centre of the Istria peninsula of Croatia; Ombla karst spring in Croatia) or a  
361 ground runoff (e.g. Cuatrociénegas of Mexico) using geophysical and geochemical methods  
362 (Bonacci, 2001; Wolaver et al., 2008). In these cases it is reliable that determined the catchment  
363 area of the ground runoff on the surface, but expensive and impracticable that the methods are  
364 applied to a greater geographical spatial scales. Therefore, this study has combined the above two  
365 advantages to delineate KW basing on the dual structure of the surface and subsurface, and this  
366 integrative delineation KW framework can be applied to map karstic catchments in multi-scales.

367

## 368 **5.2. The minimum karstic watershed unit**



369

370 In the field of topography, the key of watershed delineation is the extraction of drainage  
371 network that can be divided into different rank, accordingly, the rank of the watershed can be  
372 divided respectively (Fürst and Hörhan, 2009). Moreover, one of the most critical issues in  
373 deriving drainage networks from DEMs is the location of the channel head in the Arc-Hydrology  
374 tool (Vogt et al., 2003). Therefore, whatever a contributing area threshold to generate headwater  
375 can be defined and then the vary drainage network and watershed can be delineated.

376 However, Karst landscapes are influenced by three main factors: the geological setting, the  
377 influence of events within the Quaternary (the last c. 1.8 million years), and recent processes  
378 (usually taken to cover events within the Holocene or the last c. 10,000 years) (Viles, 2003). In  
379 some areas, with the affection from the lithology and geological tectonic movement, and the  
380 domination from the earth's crust uplift and the long-term corrosion (as described the above 3.2),  
381 runoffs often enter into ground conduits (Pitty, 1968). Then the inconsistency can be developed  
382 between the delineation watershed area by only considering the surface topography and the  
383 physical hydrological process (Fig. 4). Obviously, the watershed shouldn't be further divided in  
384 such karst areas. This study has proposed that the minimum unit of the river basin in karst regions  
385 should be the watershed whose exit is the corrosion-erosion datum, which ensures the coincident  
386 hydrological process of the dual structure of surface and subsurface.

387

### 388 **5.3. The method's applicability**

389

390 The method of delineation KW in this study has proposed karst based on the dual structure of  
391 surface and subsurface and should be used in the karst areas where a wide range of closed surface  
392 depressions, a well-developed underground drainage system, and a strong interaction between  
393 circulation of surface water and groundwater is typical (Bonacci, 2009). In contrast, (i) for the  
394 karst area covered by glaciers (e.g. northern Tibet; high alpine; cordillera), the karst solution  
395 processes are unlikely to be an important factor in karst landform development because of low  
396 solubilities and/ or low secondary porosity (Zhang 1996; Plan et al., 2009; Viles, 2003); (ii) for  
397 steep slope in karst areas (e.g. the eastern Tibet plateau), the karst hydrological processes are  
398 dominated by surface runoff and the development degree of underground karst processes is low. In



399 the above two areas, a watershed can be delineated by traditional method on the basis of the  
400 surface topography.

401 Moreover, the small watershed extracted by using the new method has a better application value  
402 in the management of regional water resources, ecological construction, and management of land  
403 utilization. On that account, this method can be utilized by fellow scientists and government  
404 managers from around the world. Furthermore, on the basis of the method proposed in this study,  
405 our subsequent study will be focused on further promotion of the level of automation in KW  
406 extraction.

407

## 408 **6. Conclusions**

409

410 In this study, we propose that, under specific eco-hydrogeological backgrounds, the traditional  
411 method of automatic extraction of watershed based merely on surface topography is inauthentic  
412 and cannot reflect the eco-hydrological process of the dual structure of the surface and subsurface  
413 accurately. Thus, a new method that is applicable for the extraction of small watersheds in karst  
414 areas is imperative. This study focuses on the eco-hydrological background of karst regions and  
415 proposes a new method for the extraction of small watershed in karst areas. The extraction of  
416 small watersheds is achieved through the following five steps: (i) automatic extraction of small  
417 watershed in the surface terrain is conducted (ATW); (ii) regional corrosion–erosion datum and  
418 exit of watershed are determined; (iii) trunk stream of the dual structure of the surface and  
419 underground in karst regions is determined; (iv) flow direction in the permeable stratum of karst  
420 carbonatite in the regions where trunk stream flows through is determined; (v) divide of ATW is  
421 corrected. In this method, vector topographic data, geological data, hydrogeological data, and data  
422 source of high-resolution remote sensing are employed. By the combined utilization of ArcGIS  
423 platform and field survey, the extraction of small KWs is completed.

424 This method is applied to one section of the tributary area (Sancha River) of the Yangtze River  
425 in China. By comparing the quantity, shape, and superimposition between the traditional method  
426 of automatic extraction and the method proposed in this study, we can conclude that a significant  
427 inconsistency exists between small watersheds extracted in karst areas by using the two methods.  
428 Furthermore, the hydrological processes in small watersheds extracted by using these two methods



429 are compared. A significant amount of errors exist in the small watershed extracted automatically.  
430 By contrast, small KWs extracted by using the new method proposed in this study can reflect the  
431 hydrological process of watersheds accurately. On the basis of the results previously presented, we  
432 deem that the minimum unit of watershed in karst areas is the watershed whose exit is the  
433 corrosion–erosion datum proposed in this study. A further subdivision of watershed may cause a  
434 significant inconsistency with the true eco-hydrological process.

435

#### 436 **Acknowledgments**

437

438 This work was supported by the 973 Program of China (2013CB956704), the National Key  
439 Technology R&D Program (2014BAB03B02), the National Natural Science Foundation of China  
440 (41461041, 41473055) and the Chinese academy of sciences strategic leading science and  
441 technology projects (XDA05070401).

442

443

#### 444 **References**

445

- 446 Ahamed, T. R.N., Rao, K.G., Murthy, J. S. R., 2002. Automatic extraction of tank outlets in a  
447 sub-watershed using digital elevation models. *Agricul. Water Man.* 57, 1-10
- 448 Bailly-Comte, V., Jourde, H., Pistre, S., 2009. Conceptualization and classification of  
449 groundwater–surface water hydrodynamic interactions in karst watersheds: Case of the karst  
450 watershed of the Coulazou River (Southern France). *J. Hydrol.* 376, 456–462
- 451 Band, L.E., 1986. Topographic partition of watersheds with digital elevation models. *Water Resour.*  
452 *Res.* 22, 15-24
- 453 Benosky, C. P., Merry, C. J., 1995. Automatic extraction of watershed characteristics using spatial  
454 analysis techniques with application to groundwater mapping. *J. Hydrol.* 173, 145-163
- 455 Bonacci, O., 2001. Analysis of the maximum discharge of karst springs. *Hydrogeology Journal.* 9,  
456 328–338
- 457 Bonacci, O., Pipan, T., Culver, D.C., 2009. A framework for karst ecohydrology. *Environ. Geol.* 56,  
458 891–900.



- 459 Doglioni, A., Simeone, V., Giustolisi, O., 2012, The activation of ephemeral streams in karst  
460 catchments of semi-arid regions. *Catena*. 99, 54-65
- 461 Fitzpatrick, F.A., 1998. Geomorphic and hydrologic responses to vegetation, climate, and base  
462 level changes, North Fish Creek, Wisconsin. University of Wisconsin-Madison
- 463 Ford, D., Williams, P., 2007. *Karst hydrogeology and geomorphology*. John Wiley & Sons Ltd,  
464 England
- 465 Fürst, J., Hörhan, T., 2009. Coding of watershed and river hierarchy to support GIS-based  
466 hydrological analyses at different scales. *Computers & Geosciences*. 35, 688-696
- 467 Gallant, J.C., Hutchinson, M.F., 2009. A Differential Equation for Specific Catchment Area.  
468 *Proceedings of Geomorphometry*. *Water Resour. Res.* 47, 143-158
- 469 García, M. J. L., Camarasa, A. M., 1999. Use of geomorphological units to improve drainage  
470 network extraction from a dem: comparison between automated extraction and  
471 photointerpretation methods in the carraixet catchment (valencia, spain). *International Journal*  
472 *of Applied Earth Observation and Geoinformation (JAG)*. 1, 187-195
- 473 Hancock, G.R., Martinez, C., Evans, K.G., Moliere, D.R., 2006. A comparison of SRTM and  
474 high-resolution digital elevation models and their use in catchment geomorphology and  
475 hydrology: Australian examples. *Earth Surface Processes Landforms*. 31, 1394-1412
- 476 Hollenhorst, T. P., Brown, T. N., Johnson, L. B., Ciborowski, J. J. H., Host, G. E., 2007. Methods  
477 for generating multi-scale watershed delineations for indicator development in great lake  
478 coastal ecosystems. *J. Great Lakes Res.* 33,13-26
- 479 Jarihani, A.A., Callow, J.N., McVicar, T.R., Van Niel, T.G., Larsen, J.R., 2015. Satellite-derived  
480 Digital Elevation Model (DEM) selection, preparation and correction for hydrodynamic  
481 modelling in large, low-gradient and data-sparse catchments. *J.Hydro.* 524, 489-506
- 482 Jensen S.K., 1991. Application of hydrology information automatically extracted from digital  
483 elevation model. *Hydrol. Proces.* 5, 31-44
- 484 Jenson, S.K., Domingue, J.O., 1988. Extracting topographic structure from digital elevation data  
485 for geographic information system analysis. *Photogrammetric Eng. Rem. Sens.* 54, 1593-1600
- 486 Jiang, Z. C., Luo, W. Q., Deng, Y., Cao, J. H., Qin, X. M., Li, Y.Q., Yang, Q.Y., 2014. The leakage  
487 of water and soil in the karst peak cluster depression and its prevention and treatment. *Acta*  
488 *Geosci. Sin.* 35,535-542 (In Chinese with English abstract)



- 489 Jiang, Z.C., Lian, Y.Q., Qin, X.Q., 2014. Rocky desertification in Southwest China: impacts,  
490 causes, and restoration. *Earth-Sci. Reviews.* 132, 1-12
- 491 Khan, A., Richards, K. S., Parker, G. T., Mcrobie, A., Mukhopadhyay, B., 2014. How large is the  
492 upper indus basin? the pitfalls of auto-delineation using dems. *J. Hydrol.* 509, 442-453
- 493 Kiss, R., 2004. Determination of drainage network in digital elevation models, utilities and  
494 limitations. *Hung. Geomath.* 2, 16–29
- 495 Li, C.F., Feng, X.Z., Zhao, R., 2003. The methods and application of automatically extracting  
496 stream network of watershed. *J. Lake Sci.* 15, 205-202 (In Chinese with English abstract)
- 497 Li, D.W., Cui, Z.J., 2004. Karst planation surface and the qinghai-xizang plateau uplift. *Quat. Sci.*  
498 24, 58-66 (In Chinese with English abstract)
- 499 Li, L., Hao, Z.C., 2003. The automated extraction of catchment properties from digital elevation  
500 models. *Advance in Earth Sci.* 18, 251-256 (In Chinese with English abstract)
- 501 Liu, Y.H., Li, X.B., 2007. Fragile eco-environment and sustainable development. The Commercial  
502 Press, Beijing, pp. Chapter 5
- 503 Majone, B., Bellin, A., Borsato, A., 2004. Runoff generation in karst catchments: multifractal  
504 analysis. *J. Hydrol.* 294, 176–195
- 505 Malard, A., Jeannin, P., Vouillamoz, J., Weber, E., 2015. An integrated approach for catchment  
506 delineation and conduit-network modeling in karst aquifers: application to a site in the Swiss  
507 tabular Jura. *Hydrogeology Journal.* DOI 10.1007/s10040-015-1287-5
- 508 Mantelli, L. R., Barbosa, J. M., Bitencourt, M. D., 2011. Assessing ecological risk through  
509 automated drainage extraction and watershed delineation. *Ecol. Inform.* 6, 325–331
- 510 Marks, D., Dozier, J., Frew, J., 1984. Automated basin delineation from digital elevation data.  
511 *Geo-Processing.* 2, 299-311
- 512 Martz, L.W., Garbrecht, J., 1999. An outlet breaching algorithm for the treatment of closed  
513 depressions in a raster DEM. *Compu. & Geosci.* 25, 835-844
- 514 Mayaud, C., Wagner, T., Benischke, R., Birk, S., 2014. Single event time series analysis in a  
515 binary karst catchment evaluated using a groundwater model (Lurbach system, Austria). *J.*  
516 *Hydrol.* 511, 628–639
- 517 McCormack, T., Gill, L.W., Naughton, O., Johnston, P.M., 2014, Quantification of  
518 submarine/intertidal groundwater discharge and nutrient loading from a lowland karst



- 519 catchment. *J. Hydrol.* 519, 2318-2330
- 520 Meng, H.H., Wang, L.C., 2010 Advance in karst hydrological model. *Progress in Geography.* 29,  
521 1311-1318 (In Chinese with English abstract)
- 522 Navas, A., López-Vicente, M., Gaspar, L., Machín, J., 2013. Assessing soil redistribution in a  
523 complex karst catchment using fallout <sup>137</sup>Cs and GIS. *Geomor.* 196, 231-241
- 524 Nico, G., David, D., 2007. *Methods in karst hydrogeology.* Taylor & Francis Group, London
- 525 Nikolakopoulos, K.G., Kamaratakis, E.K., Chrysoulakis, N., 2006. SRTM vs ASTER elevation  
526 products. Comparison for two regions in Crete, Greece. *Rem. Sens.* 27, 4819–4838
- 527 NRC (National Research Council), 1999. *New strategies for America's watersheds.* National  
528 Academy Press, pp.1-4
- 529 O'Callaghan, J.F., Mark, D.M., 1984. The extraction of drainage networks from digital elevation  
530 data. *Comput. Vision Graphics Image Process.* 28, 323-344
- 531 Peng, T., Wang, S. J., 2012. Effects of land use, land cover and rainfall regimes on the surface  
532 runoff and soil loss on karst slopes in southwest china. *Catena.* 90, 53–62.
- 533 Peucker, T.K., Douglas, D.H., 1975. Detection of surface-specific points by local parallel  
534 processing of discrete terrain elevation data. *Comput. Graph. Image Process.* 4, 375-387
- 535 Pitty, A.F., 1968. Calcium carbonate content of karst water in relation to flow-through time. *Nature.*  
536 5132, 939-940
- 537 Plan, L., Decker, K., Faber, R., Wagreich, M., Grasmann, B., 2009. Karst morphology and  
538 groundwater vulnerability of high alpine karst plateaus. *Environ. Geol.* 58, 285-297
- 539 Qiu, L.J., Zheng, F.L., 2012. Effects of dem resolution and watershed subdivision on hydrological  
540 simulation in the xingzihe watershed. *Acta Ecol. Sin.* 32, 3754-3763
- 541 Qiu, L.J., Zheng, F.L., Yin, R.S., 2012. Effects of DEM resolution and watershed subdivision on  
542 hydrological simulation in the Xingzihe watershed. *Acta Ecol. Sin.* 32, 3754-3763 (In  
543 Chinese with English abstract)
- 544 Ravbar, N., Goldscheider, N., 2009. Comparative application of four methods of groundwater  
545 vulnerability mapping in a Slovene karst catchment. *Hydrogeology Journal.* 17, 725–733
- 546 Rimmer, A., Salingar, Y., 2006. Modelling precipitation-streamflow processes in karst basin: The  
547 case of the Jordan River sources, Israel. *J. Hydrol.* 331, 524– 542
- 548 Seyler, F., Muller, F., Cochonneau, G., Guimarães, L., Guyot, J.L., 2009, Watershed delineation



- 549 for the Amazon sub-basin system using GTOPO30 DEM and a drainage network extracted  
550 from JERS SAR images. *Hydrol. Process.* 23, 3173–3185
- 551 Soille, P. J., Ansoult, M. M., 1990. Automated basin delineation from digital elevation models  
552 using mathematical morphology. *Signal Process.* 20, 171-182
- 553 Tarboton, D. G., Bras, R. L., Rodriguez-Iturbe, I., 1991. On the extraction of channel networks  
554 from digital elevation data. *Hydrol. Proces.* 5, 81-100
- 555 Verdin, K.L., Verdin, J.P., 1999. A topological system for delineation and codification of the  
556 Earth's river basins. *J. Hydrol.* 218, 1-12
- 557 Viles, H.A., 2003. Conceptual modeling of the impacts of climate change on karst geomorphology  
558 in the UK and Ireland. *J. Nat. Conserv.* 11, 59-66
- 559 Vogt, J. V., Colombo, R., Bertolo, F., 2003. Deriving drainage networks and catchment boundaries:  
560 a new methodology combining digital elevation data and environmental characteristics.  
561 *Geomor.* 53, 281-298
- 562 Wang, S.J., Li, Y.B., Li, R.L., 2004. Karst rocky desertification: formation background, evolution  
563 and comprehensive taming. *Quat. Sci.* 23, 657-666 (In Chinese with English abstract)
- 564 Wicks, C.M., 1997. Origins of groundwater in a Fluviokarst basin: Bonne Femme basin in central  
565 Missouri, USA. *Hydrogeology Journal.* 5, 89–96
- 566 Wilson, J.P., Gallant, J.C., 2000. *Terrain analysis principles and applications.* John Wiley & Sons.  
567 Canada, pp. Chapter 1
- 568 Wolaver, B.D., Sharp Jr., J.M., Rodriguez, J.M., Ibarra Flores, J.C., 2008. Delineation of Regional  
569 Arid Karstic Aquifers: An Integrative Data Approach. *Ground Water.* 46, 396-413
- 570 Xiao, H., Xiong, K.N., Zhang, H., Zhang, Q.Z., 2014. Research progress for karst rocky  
571 desertification control models, *China Popul., Resour. and Environ.* 25, 330-334 (In Chinese  
572 with English abstract)
- 573 Xiong, K.N., Li, J., Long, M.Z., 2014. Features of soil and water loss and key issues in  
574 demonstration areas for combating karst rocky desertification. *Acta Geogr. Sin.* 67, 877-888  
575 (In Chinese with English abstract)
- 576 Yan, D.X., 1997. Rock desertification in the subtropical karst of South China. *Zeitschrift für*  
577 *Geomorphologie.* 108, 81-90
- 578 Yang, M.D., 1982. The geomorphological regularities of karst water occurrences in Guizhou plateau.



- 579 Carsologica Sin. 2, 81-91 (In Chinese with English abstract)
- 580 Yue, F.J., Li, S.L., Liu, C.Q., Lang, Y.C., Ding, H., 2015. Sources and transport of nitrate  
581 constrained by the isotopic technique in a karst catchment: an example from Southwest China.  
582 Hydrol. Process. 29, 1883–1893
- 583 Zhang, D., 1996. A morphological analysis of Tibetan limestone pinnacles: Are they remnants of  
584 tropical karst towers and cones? Geomor. 15, 79-91
- 585 Zhang, J. F., Feng, X. B., Yan, H. Y., Guo, Y. N., Meng, B., Yao, H., 2011. Spatial and temporal  
586 distribution of mercury species in water in yelanghu reservoir. Chinese J. Ecol. 30, 969-975  
587 (In Chinese with English abstract)
- 588